

Forest Kernel Balancing Weights: Outcome-Guided Features for Causal Inference*

Andy A. Shen[†] Eli Ben-Michael[‡] Avi Feller[§] Luke Keele[¶] Jared Murray^{||}

December 15, 2025

Abstract

While balancing covariates between groups is central for observational causal inference, selecting which features to balance remains a challenging problem. Kernel balancing is a promising approach that first estimates a kernel that captures similarity across units and then balances a (possibly low-dimensional) summary of that kernel, indirectly learning important features to balance. In this paper, we propose *forest kernel balancing*, which leverages the underappreciated fact that tree-based machine learning models, namely random forests and Bayesian additive regression trees (BART), implicitly estimate a kernel based on the co-occurrence of observations in the same terminal leaf node. Thus, even though the resulting kernel is solely a function of baseline features, the selected nonlinearities and other interactions are important for predicting the outcome—and therefore are important for addressing confounding. Through simulations and applied illustrations, we show that forest kernel balancing leads to meaningful computational and statistical improvement relative to standard kernel methods, which do not incorporate outcome information when learning features.

Keywords: causal inference; observational studies; weighting, inverse probability weighting, balancing weights

*This research is supported by the Institute of Education Sciences, U.S. Department of Education, through Grants R305D210014 and R305D240036. Andy Shen is supported by the National Science Foundation (NSF) Graduate Research Fellowship under Grant No. 2146752. The opinions expressed are those of the authors and do not represent views of the funding institutions.

[†]University of California, Berkeley, Email: aashen@berkeley.edu

[‡]Carnegie Mellon University, Email: ebenmichael@cmu.edu

[§]University of California, Berkeley, Email: afeller@berkeley.edu

[¶]University of Pennsylvania, Email: luke.keele@gmail.com

^{||}University of Texas, Austin, Email: jared.murray@mccombs.utexas.edu

1 Introduction

A central goal of observational study design is to achieve *covariate balance*, which ensures that treated and control groups are comparable on observed characteristics (Ben-Michael et al., 2021). Weighting methods accomplish this by, for example, re-weighting the control group to have a comparable covariate distribution to the treated group, such as via inverse propensity score weighting (IPW). However, choosing which features to re-weight can be challenging: failing to capture important nonlinearities or other complex relationships can lead to bias.

Kernel balancing is a promising data-driven approach that uses kernel methods to indirectly learn a (possibly infinite) set of features to balance (Wong and Chan, 2018; Hazlett, 2020; Kim et al., 2024). The key idea is to first compute a kernel matrix \mathbf{K} and then use existing weighting approaches to balance a low-dimensional summary of \mathbf{K} . Kernel methods are typically *design based*: they encode similarity between units based on a fixed kernel derived from baseline features only. While such kernels can capture complex relationships between covariates, they may fail to reflect nonlinearities and other relationships that are important for predicting the outcome—and therefore that are important for addressing confounding.

In this paper, we propose *forest kernel balancing*, in which we use outcome information to learn the kernel matrix \mathbf{K} to balance. In particular, we leverage the fact that tree-based machine learning models, namely random forests (RF) and Bayesian additive regression trees (BART), implicitly estimate a kernel based on the co-occurrence of observations in the same terminal leaf node (Breiman, 2000; Scornet, 2016; Hill et al., 2020). Thus, while \mathbf{K} is still solely a function of the baseline features, incorporating the outcome into learning \mathbf{K} ensures that these relationships are pertinent to the outcome, which appropriately captures more sources of confounding (Jin and Zubizarreta, 2025). We conduct extensive simulation studies and show that forest kernel balancing reduces bias and RMSE compared to design-based kernel existing methods. We then demonstrate this approach in practice with an applied illustration to an educational training program (Keller et al., 2025) and an observational study of the effects of child soldiering (Blattman and Annan, 2010).

This paper builds on an extensive literature on kernel methods implied by random forests and related tree-based methods, as well as an emerging literature on leveraging outcome information to improve observational study design (Jin and Zubizarreta, 2025). See Breiman (2000) for an early connection and Scornet (2016); Balog et al. (2016) for more detailed discussion. Separately, Lin and Jeon (2006) provide an early interpretation of random forests as a weighted nearest neighbor methods. For BART, the connection to kernel methods is typically via BART’s representation as a Gaussian process; see Hill et al. (2020) for a review.

Our paper is structured as follows: Section 2 provides our setup and background on different weighting approaches. Section 3 introduces forest kernels and kernel balancing. Section 4 compares performance via a series of simulations. Section 5 demonstrates the performance of our kernel with two empirical case studies. Section 6 concludes. The code to reproduce our findings can be found

at the following link: <https://github.com/aashen12/forest-kbal>.

2 Background

2.1 Notation, assumptions, and estimands

We assume we have a sample of units $i = 1, \dots, n$, drawn i.i.d. from some population. We denote a binary treatment Z_i , where $Z_i = 1$ and $Z_i = 0$ corresponds to the treated and control conditions, respectively; n_1 and n_0 denote the corresponding number of treated and control units. We let Y_i denote the observed outcome, and we use the potential outcomes framework, where each unit has two potential responses $Y_i(1)$ and $Y_i(0)$, corresponding to their respective response under treatment and control. The observed outcome is $Y_i = Z_i Y_i(1) + (1 - Z_i) Y_i(0)$. Finally, we invoke the Stable Unit Treatment Value Assumption (Rubin, 1986), which implies no hidden forms of treatment and no interference across units. To reduce notational complexity, we will drop the i subscript when taking expectations and probabilities. We use X_i to denote a vector of baseline covariates. Throughout, we will make use of the *propensity score*, the probability of receiving treatment conditional on the baseline covariates, which we denote as: $e(x) = \mathbb{P}(Z = 1 | X = x)$.

Our estimand of interest is the *average treatment effect on the treated (ATT)*, the average difference in outcomes for those individuals in the population actually exposed to treatment:¹

$$\tau = \mathbb{E}[Y(1) - Y(0) | Z = 1] = \mathbb{E}[Y(1) | Z = 1] - \mathbb{E}[Y(0) | Z = 1]. \quad (1)$$

For individuals exposed to treatment, we directly observe $Y(1)$ and therefore can directly estimate the mean outcome under treatment for this group, $\mu_1 \equiv \mathbb{E}[Y(1) | Z = 1]$, such as via the sample average outcome among the treated. The challenge is then to estimate the average counterfactual outcomes for this group, $\mu_0 \equiv \mathbb{E}[Y(0) | Z = 1]$, which will be the focus of our discussion.

We require two additional assumptions to identify μ_0 . First, we assume that treatment assignment is ignorable, conditional on the covariates X (i.e., no unmeasured confounding):

$$Y(0), Y(1) \perp\!\!\!\perp Z | X.$$

Second, we assume there is overlap in the covariate distributions between the treated and control groups: for the ATT, this assumption requires that no units are deterministically treated, i.e. $e(x) < 1$ for each x in the population.

Under these assumptions, the average counterfactual outcome $\mathbb{E}[Y(0) | Z = 1]$ (and therefore the

¹While our work focuses on the ATT for clarity, the proposed methodology can be extended to other common estimands, such as the average treatment effect (ATE) or the average treatment effect for the overlap population (ATO).

ATT) is identified as a function of the propensity score and observed outcomes:

$$\mathbb{E}[Y(0) | Z = 1] = \mathbb{E}\left[\underbrace{\frac{e(X)}{1 - e(X)} Y}_{\text{IPW}} | X, Z = 0\right],$$

where $e(x)/(1 - e(x))$ are the “inverse” propensity score weights.

2.2 Estimating inverse propensity score weights via balancing

Our goal is to construct a weighting estimator for the mean counterfactual outcome for the treated group, μ_0 . With known propensity score $e(x)$, we can estimate this unobserved portion of the ATT via a weighted average of the outcomes in the control group:

$$\hat{\mu}_0 = \sum_{i=1}^n (1 - Z_i) w_i Y_i. \quad (2)$$

Based on the identification formula above, we should set w_i to equal the inverse propensity score weights, $w_i = \frac{e(x_i)}{1 - e(x_i)}$. The key challenge is to estimate these inverse propensity score weights when the propensity score is not known. Traditional IPW first estimates the propensity score $e(x)$ and then plugs the estimated values $\hat{e}(x)$ into the analytic form for the weights. This approach, however, can lead to unstable estimates and poor implied covariate balance with even moderate dimensional covariates x : since $e(x)$ is in the denominator, errors in $\hat{e}(x) - e(x)$ can cause the estimator to “blow up” (see [Ben-Michael et al., 2021](#)).

Instead we focus on methods that estimate inverse propensity score weights directly. To motivate this approach, note that under standard identifying conditions we can rewrite the observed outcome for unit i as

$$Y_i = (1 - Z_i) Y_i(0) + Z_i Y_i(1) = \mu_0(x_i) + Z_i \tau_i + \varepsilon_i,$$

where

$$\mu_0(x) \equiv \mathbb{E}[Y(0) | X = x] = \mathbb{E}[Y | X = x, Z = 0]$$

is the potential outcome function; $\tau_i \equiv Y_i(1) - Y_i(0)$ is the individual-level treatment effect; and ε_i is conditionally mean zero noise. We can then write a weighting estimator of the unobserved counterfactual mean μ_0 :

$$\hat{\mu}_0 = \sum_{i=1}^n (1 - Z_i) w_i y_i = \frac{1}{n_1} \sum_{i=1}^n Z_i \mu_0(x_i) + \underbrace{\left(\sum_{i=1}^n (1 - Z_i) w_i \mu_0(x_i) - \frac{1}{n_1} \sum_{i=1}^n Z_i \mu_0(x_i) \right)}_{\text{imbalance in } \mu_0(x)} + \text{noise}, \quad (3)$$

where we add and subtract $\frac{1}{n_1} \sum_{i=1}^n Z_i \mu_0(x_i)$, a sample analogue of the unobserved counterfactual mean, and where the noise term is a mean-zero weighted sum of the ε_i terms. The core task of a weighting estimator is then to control the imbalance term. If we knew the true potential outcome

function $\mu_0(x)$, we could simply find weights to balance this quantity.

Balancing weights. Unfortunately, we do not know $\mu_0(x)$. Instead, we can leverage an important property of inverse propensity score weights: they are the unique weights that balance *any* (integrable) function between the treated and control groups, including the unknown $\mu_0(x)$. The space of all integrable functions is very large, and so balancing weights estimators posit a *function class* for $\mu_0(\cdot)$ that restricts the model in some way. There is a direct correspondence between the choice of function class and the form of covariates or their transformations that should be balanced (Ben-Michael et al., 2021). As a leading example, if $\mu_0(x) = x^\top \beta$ is linear in the covariates x , then the resulting imbalance term is controlled by the difference between the average value of the covariates x in the treated group and the *weighted* average in the control group.

In practice, it is useful to consider weights that achieve *approximate* balance and also penalize the dispersion of the weights. Following the developments in Ben-Michael et al. (2023, 2024); Keele et al. (2023, 2025), we consider the following “linear” balancing weights objective function:

$$\min_{w \in \Delta^n} \underbrace{\left\| \sum_{i=1}^n (1 - Z_i) w_i \mathbf{X}_i - \frac{1}{n_1} \sum_{i=1}^n Z_i \mathbf{X}_i \right\|_2^2}_{\text{imbalance}} + \lambda \underbrace{\sum_{i=1}^n w_i^2}_{\text{dispersion}}, \quad (4)$$

where we pre-process each covariate X_k to have mean 0 and variance 1. We can identify this objective as representing a bias-variance tradeoff, where the leading term represents worst-case confounding over functions linear in x and the penalty reduces the dispersion of the weights (Ben-Michael et al., 2023; Keele et al., 2025; Hirshberg and Wager, 2021; Ben-Michael and Keele, 2023). Following Hirshberg and Wager (2021) and Ben-Michael and Keele (2023), we set this hyperparameter to the residual variance from a regression of the outcome (scaled to have mean zero and variance one) on covariates within the control group. We also restrict the weights to be on the simplex $w \in \Delta^n$ (i.e., they are non-negative and sum to 1), though we can relax this restriction (Arbour et al., 2025).²

Different approaches to balancing weights make different choices about these functions — e.g., replacing the 2-norm of imbalance with a stronger norm — though they all follow the same principle of minimizing a combination of imbalance and weight dispersion/complexity. See Zubizarreta (2015); Wang and Zubizarreta (2020); Athey et al. (2018); Tan (2020) for alternative approaches. Our forest kernel balancing proposal is easily adapted to alternative balancing weight estimators.

Feature maps. Other model classes induce additional balance terms, e.g. positing that $\mu_0(\cdot)$ is a quadratic model corresponds to measuring imbalance across all covariates and their second-order

²Note that in this formulation, weights on treated units are also part of the vector w , but because they do not appear in the imbalance objective they are regularized to zero if $\lambda > 0$.

interactions. Generally, we can denote this via a *feature vector* $\phi : \mathcal{X} \rightarrow \mathbb{R}^q$:

$$X \rightarrow \phi(X).$$

For example, if ϕ includes quadratic terms, then the balancing objective aims to balance the first two moments of the covariates.

The goal of choosing features $\phi(x)$ is to construct a rich set of functions $\phi(x) = (\phi_1(x), \phi_2(x), \dots)$ that is sufficiently large so that it can adequately represent $\mu_0(\cdot)$, i.e. $\mu_0(x) \approx \phi(x)^\top \beta$, but not so large that achieving good balance in a finite sample is too difficult (Ben-Michael et al., 2021); see also Austin et al. (2007); Austin and Stuart (2015) for extensive discussion.³ Given this feature map ϕ we can then consider a modified balancing weights objective:

$$\min_{w \in \Delta^n} \underbrace{\left\| \sum_{i=1}^n (1 - Z_i) w_i \phi(\mathbf{X}_i) - \frac{1}{n_1} \sum_{i=1}^n Z_i \phi(\mathbf{X}_i) \right\|_2^2}_{\text{imbalance in } \phi(x)} + \lambda \underbrace{\sum_{i=1}^n w_i^2}_{\text{dispersion}}. \quad (5)$$

Once again we have an issue: selecting appropriate features $\phi(x)$ is challenging because we do not know $\mu_0(x)$. Here we can construct the feature map by hand, or, as we discuss next, implicitly by specifying a kernel function.

2.3 Kernels and kernel balancing

Kernel balancing is a generalization of balancing weights that minimizes an objective like (5) with a (potentially) infinite number of features, using the “kernel trick” to avoid explicitly forming the features. We briefly review kernels and kernel balancing here, focusing on Mercer and generic inner-product kernels, which will cover all of our use cases and most of the kernel balancing literature.

A *kernel* is a positive definite function $k(\cdot, \cdot) : \mathcal{X} \times \mathcal{X} \mapsto \mathbb{R}$ that encodes similarity between observations based on their covariates. By the reproducing property:

$$k(x_i, x_j) = \langle k(\cdot, x_i), k(\cdot, x_j) \rangle_{\mathcal{H}},$$

where the inner product is in the reproducing kernel Hilbert space (RKHS) associated with the kernel \mathcal{H} . For many common kernels, we can make these features explicit by choosing an infinite-dimensional map $\phi(x) : \mathcal{X} \rightarrow \mathbb{R}^\infty$ such that

$$k(x_i x_j) = \langle \phi(x_i), \phi(x_j) \rangle_2 = \sum_{h=1}^{\infty} \phi_h(x_i) \phi_h(x_j).$$

³An alternative motivation for selecting $\phi(x)$ is to instead find functions that adequately represent the true inverse propensity score weights themselves. See, for example, Jin and Zubizarreta (2025).

We can therefore think of a kernel as encoding a (non-unique) transformation of the original covariates, analogous to augmenting our original variables with polynomial expansions, interactions, or other transformations.

The famous *kernel trick* then allows us to substitute $\phi(x)$ for x in the imbalance component of the objective function in Equation (4), even with infinite-dimensional $\phi(x)$, without ever explicitly forming the feature vectors $\phi(x)$ themselves. For any two $a_0, a_1 \in \mathbb{R}^n$ we have

$$\left\langle \sum_i a_{0i} \phi(x_i), \sum_j a_{1j} \phi(x_j) \right\rangle_2 = \sum_{i,j} a_{0i} a_{0j} \phi(x_i)^\top \phi(x_j) = \sum_{i,j} a_{0i} a_{0j} k(x_i, x_j).$$

We can then write the imbalance term in Equation (5) as

$$\left\| \sum_{i=1}^n (1 - Z_i) w_i \phi(\mathbf{X}_i) - \frac{1}{n} \sum_{i=1}^n Z_i \phi(\mathbf{X}_i) \right\|_2^2 = a_0^\top \mathbf{K} a_0 + a_1^\top \mathbf{K} a_1 - 2 a_0^\top \mathbf{K} a_1,$$

$$a_{0i} = (1 - Z_i) w_i, \quad a_{1i} = Z_i / n.$$

This is (up to scaling and regularization) an instantiation of *kernel mean matching* (Gretton et al., 2009), where we learn weights that shift the distribution of features in the controls to match the distribution of features among treated units.

Approximate kernels and spectral truncation. While many kernels implicitly induce infinite-dimensional feature vectors, in practice at most n of these are realized in any given sample (and typically the effective dimension is much lower). That is,

$$\mathbf{K} = \Phi \Phi^\top \approx \hat{\Phi} \hat{\Phi}^\top,$$

where $\hat{\phi}(x)$ is an approximate feature vector of length $r \ll q$. An important special case of this is the *spectral approximation*; see Wong and Chan (2018); Hazlett (2020); Kim et al. (2024); Hartman et al. (2024). Let $\mathbf{K} = \mathbf{U} \mathbf{D} \mathbf{U}^\top$ be the eigendecomposition of the kernel matrix, where $\mathbf{D} = \text{diag}(\sigma_1^2, \dots, \sigma_n^2)$. The spectral approach retains the top r principal components of \mathbf{K} , scaled by their singular values: $\hat{\phi}_k(x) = \sigma_k U_k$ for $k = 1, \dots, r$. We can then minimize imbalance in these (scaled) principal components directly. Imbalance in the trailing principal components (i.e., $k = r+1, \dots, n$) is small in absolute value because the corresponding singular values are small. As a result, using the low-rank approximation $\hat{\Phi}$ instead of Φ can significantly enhance computational efficiency, and potentially enhance statistical efficiency, with only minimal additional imbalance.

Choosing r is therefore an important hyperparameter with many kernel balancing methods. To do so, Hazlett (2020) defines a “worst-case” bias bound and chooses r to minimize this bias bound—but also demonstrates that estimation accuracy is relatively insensitive to this choice, so long as r is not too extreme. We report results over a grid of r values and proceed conditionally on the selected

value, noting that any conventional selection rule can be used and the subsequent weighting and estimation steps are unchanged.

Kernel choices. The last key ingredient for kernel balancing is specifying the kernel itself, typically in addition to the spectral truncation considered above. We focus on two common choices: *polynomial* and *Gaussian* kernels.

In a polynomial kernel, the features are simply a polynomial expansion of the original covariates:

$$k(x_i, x_j) = (x_i^\top \Sigma x_j + c)^d,$$

where c is a constant that balances higher and lower order polynomial terms, d is the degree of the polynomial, and Σ is a $p \times p$ matrix (used, for example, to whiten the original variables). Expanding the kernel and collecting terms one can show that the corresponding feature map comprises a d -degree polynomial transformation of the original covariates. While this setup is quite general, it is useful to focus on the simplified case of the *linear kernel* with $c = 0, d = 1, \Sigma = \mathbb{I}$: $k(x_i, x_j) = x_i^\top x_j$. This exactly recovers the linear balancing weights problem introduced above (where we can modify Σ to recover standardization).

The most common alternative in kernel balancing is the *Gaussian* or *radial basis function* kernel (Wong and Chan, 2018; Hazlett, 2020; Kim et al., 2024; Hartman et al., 2024):

$$k(x_i, x_j) = \exp(-\|x_i - x_j\|_2^2/b),$$

where b is the kernel bandwidth (a hyperparameter to be tuned) and x_i and x_j are scaled to have zero mean and variance 1. The Gaussian kernel is more flexible than the linear kernel and can approximate a wide class of functions while remaining an intuitive measure of similarity: similar covariate profiles receive kernel values closer to one, and increasing b captures more global patterns of similarity. In terms of the implied feature map $\phi(x)$, increasing b puts higher weight on smooth, low-frequency features while decreasing b puts higher weight on more irregular functions. There are many approaches for choosing bandwidth b , such as the value that produces maximal variance in \mathbf{K} (Hartman et al., 2024) or the rank of \mathbf{X} (Hazlett, 2020; Kim et al., 2024).

Combining kernels. Finally, it is often useful to balance both the raw covariates in addition to their feature space representation; see the “mean-first” procedure from Hartman et al. (2024). This corresponds to constructing a new kernel:

$$k(x_i, x_j) = x_i^\top \Sigma x_j + k_0(x_i, x_j),$$

the sum of a degree 1 (linear) polynomial kernel and another (e.g., Gaussian) kernel k_0 , either in its original form or using a spectral approximation. Practically this combined kernel amounts to modifying the imbalance term in Equation (5) to concatenate the vector of raw covariates (columns

of \mathbf{X}) and the re-scaled principal components of \mathbf{K} , $\sigma_k U_k$.

A key practical consideration is the relative scale of the two sets of features, which implicitly defines their relative importance in the squared distance balance metric used in Equation (5). As a default, we propose to normalize each “block” to have equal overall variance. In particular, we standardize X to have mean 0 and variance $1/p$, where p is the number of raw covariates; then $\sum_k \text{var}(X_k) = 1$. Using the spectral approximation for \mathbf{K} , we similarly re-scale the variance of each principal component so that the variances across the r components also sum to one: the variance of principal component j is $\sigma_j^2 / \sqrt{\sum_{i=1}^r \sigma_i^2}$ (instead of σ_j^2). This “block normalization” treats the raw covariates and kernel principal components as equally important *in aggregate* while preserving the relative importance of the principal components rather than flattening them. This way, neither the raw covariates nor the kernel features dominate the balancing weight objective function (5) and each kernel feature still maintains its importance in terms of explained variance. In practice, the total variance allocated to each block (raw or kernel) can be determined via an additional hyperparameter. While we choose equal weighting below, any choice is compatible with our framework.

Learning what to balance and the limits of design-based kernels. As we discuss in Section 2.2, the goal of choosing features $\phi(x)$ is to construct a sufficiently rich set of functions $\phi(x) = (\phi_1(x), \phi_2(x), \dots)$ such that we can approximate the true potential outcome function, $\mu_0(x) \approx \phi(x)^\top \beta$. Choosing $\phi(x)$ via a kernel, however, does not “solve” the problem of what to balance: we have simply exchanged hand-selected features for the specification of a kernel family and their parameters, which is typically more opaque. Without strong subject matter knowledge, assessing the trade-offs between kernel choices can be difficult. Moreover, commonly used kernels, including linear, polynomial and Gaussian kernels can be sensitive to transformations of the data: kernel weights based on similarity in income can be wildly different from weights based on similarity in the logarithm of income. The bandwidth in a Gaussian kernel is also not invariant to nonlinear transformations of the inputs.

More broadly, the kernel balancing framework thus far is fully *design-based*, meaning that the kernel matrix and corresponding weights are constructed using only baseline covariates. Design-based methods are appealing because they mirror the logic of randomized trials in which treatment assignment precedes outcomes. However, features constructed solely from covariate-driven kernels may be insufficient for approximating $\mu_0(x)$.

Our main proposal, which we turn to next, is to instead use outcome information to learn important features to balance; see also [Jin and Zubizarreta \(2025\)](#). In particular, we propose learning forest-based kernels, coupled with data splitting to preserve valid inference, tuned using outcome data to help learn a relevant feature representation.

3 Forest Kernel Balancing

Our main contribution is to extend kernel balancing by replacing design-based kernels with outcome-guided kernels derived from tree-based machine learning methods, known as *forest kernels*. We consider two popular choices: random forests (RF) and Bayesian additive regression trees (BART). Using outcome data helps target a relevant basis by focusing attention on feature representations that are highly correlated with outcomes. Using tree-based kernels also makes kernel balancing more robust: unlike linear and Gaussian kernels, forest kernels are largely invariant to marginal transformations of the covariates and robust to outlying observations (Breiman, 2001; Lin and Jeon, 2006). We begin by describing forest kernels in general and the implied kernels of RF and BART in particular. We then turn to broader implementation issues.

3.1 Forest Kernels

Tree ensemble methods like random forests, gradient boosted trees, and Bayesian additive regression trees (BART) implicitly define a similarity metric — a kernel — over their input spaces. There is a large literature in machine learning and statistics on such kernels and their properties (Breiman, 2000; Lin and Jeon, 2006; Scornet, 2016; Balog et al., 2016; Hill et al., 2020). We briefly review key results here.

Beginning with a single tree, Figure 1 shows a binary decision tree (a), which implies a partition of covariate space (b). The tree-based features are simply dummy variables for each leaf (c). The implied kernel is the inner product of these:

$$k(x_i, x_j) = \phi(x_i)^\top \phi(x_j) = I(i, j),$$

where

$$I(i, j) = \begin{cases} 1 & \text{if } i \text{ and } j \text{ share a leaf node} \\ 0 & \text{otherwise.} \end{cases}$$

Mean-balancing the implied feature map is equivalent to reweighting the control observations to produce a weighted histogram over the partition in Figure 1b that matches the histogram of treated observations.

A forest is the average over many tree predictions, and accordingly a forest kernel is just the average over many single-tree kernels:

$$k(x_i, x_i) = \frac{1}{T} \sum_{t=1}^T k_t(x_i, x_i) = \frac{1}{T} \sum_{t=1}^T I_t(x_i, x_i) = p_{ii}, \quad (6)$$

where p_{ii} is the proportion of trees in which observations i and j share a leaf. The implied feature map is the concatenation of all the single-tree feature maps scaled by $1/\sqrt{T}$. While features within

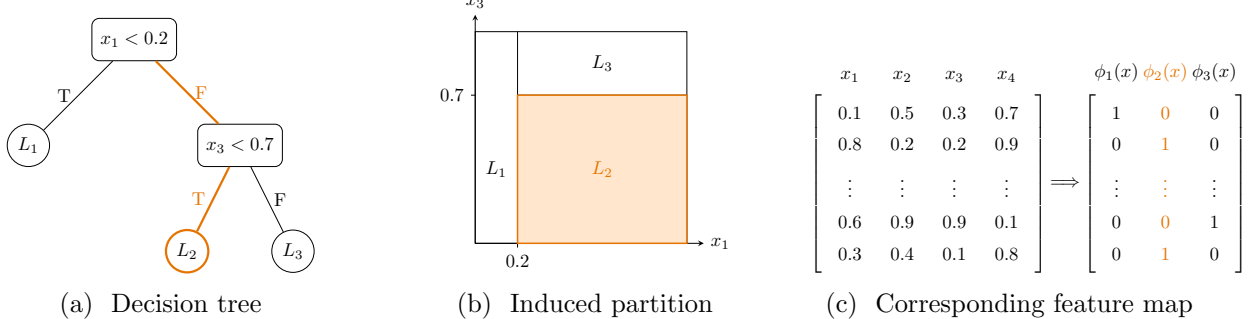


Figure 1: Illustration of the feature map implied by decision trees. (A) A single decision tree, with one path highlighted; (b) the induced partition of covariate space; and (c) the corresponding feature map $\phi(x)$. Under a single tree, points in the same partition (leaf of the decision tree) are perfectly similar and points in distinct partitions are perfectly dissimilar. In an ensemble of trees (a forest), the proportion of trees in which two points share a partition defines their similarity, and the corresponding kernel function.

a tree are orthogonal, even wildly different trees can produce correlated features, especially when the original variables are correlated. So a large tree ensemble will still often produce a kernel with small effective dimension. This motivates the spectral approximations we use below.

The ultimate kernel representation will depend on the size of the tree ensemble, the geometry of the trees in the ensemble, and the process by which they are grown. We consider random forest and BART kernels, which produce tree ensembles in markedly different ways. Both, however, use both outcome and covariate information to construct trees and implied features that are predictive of outcomes.

Random Forest Kernel. Random forests are a widely used ensemble learning method that constructs a collection of decision trees (a “forest”), each trained on a bootstrap sample of the data with random subsets of covariates selected at each split (Breiman, 2001). By averaging over many trees, this procedure avoids overfitting and reduces variance, often achieving strong predictive performance (Bühlmann and Yu, 2002; Biau and Scornet, 2016; Agarwal et al., 2023). Random forests are popular in part because they are easy to implement, require minimal tuning, and can adapt to relationships in the data that are nonlinear and complex (Agarwal et al., 2023). Random forests have been used extensively in causal inference, including as a core estimation component for heterogeneous treatment effects (Athey and Imbens, 2016; Wager and Athey, 2018) and propensity scores (Welz et al., 2024; Keele et al., 2025). The implied kernel has the same average-of-many-single-trees form as Equation (6):

$$\mathbf{K}_{ij}^{\text{rf}} = \mathbf{K}_{ji}^{\text{rf}} = \frac{1}{T} \sum_{t=1}^T I_t(x_i, x_j).$$

The trees in a random forest ensemble are typically grown very deep, resulting in fine partitions.

The bootstrap resampling and variable subsampling at each step of the random forest algorithm (along with additional tuning parameters like maximum depth of the trees) limit just how fine the partition can get and reduce correlation across the trees in the ensemble.

BART Kernel. Like random forests, BART has proved popular for applied research, with strong empirical performance across a range of tasks, especially when used for causal inference; see [Hill et al. \(2020\)](#) for a comprehensive review. Unlike RF, BART is an ensemble of small trees, more similar in spirit to boosted trees than random forests. Unlike boosting, however, the “Bayesian backfitting” MCMC algorithm for BART fixes a total number of trees (typically 200) and updates them stochastically in Metropolis-Hastings steps, biasing the trees toward feature representations that best predict outcomes but still randomly exploring a full posterior distribution over tree structures.

One output of the BART MCMC algorithm is a set of posterior draws of tree structures. For B posterior draws we take these as defining our BART kernel via

$$\mathbf{K}_{ij}^{\text{bart}} = \mathbf{K}_{ji}^{\text{bart}} = \frac{1}{BT} \sum_{b=1}^B \sum_{t=1}^T I_{bt}(i, j),$$

where $I_{bt}(i, j)$ denotes leaf co-membership for i and j in tree t in posterior draw b . Again, there is significant redundancy in this representation, both across trees within a posterior sample (since two shallow trees often produce correlated feature representations) and across posterior samples (which generally feature small changes so a subset of trees from iteration to iteration). This redundancy further motivates using a spectral approximation.

Comparison of forest kernels. Despite their similar structure, the tree geometries and differences between RF and BART can lead to meaningfully different kernels. Figure 2 illustrates one example of how these kernels compare (2a). For comparison, we also illustrate how the forest kernels compare with the Gaussian kernel (2b and 2c). The figure comes from a single realization of the data-generating process (DGP) outlined in Section 4 and is shown only to build intuition for geometries induced by these kernels in a given sample. Here we randomly sample one treated unit i from the observed analysis and plot its kernel values $k(i, j)$ where $j \neq i$.

Figure 2 shows that the all three kernels are generally correlated for this particular draw of target unit i . The figure, however, also illustrates key differences in how the two forest kernels encode similarity. This instance of RF is based on a smaller number of deeper trees where most pairs are unlikely to co-occur, producing a sparse, localized kernel. BART, by contrast, is a sum of many shallow, weak trees with partitions that often overlap. Pairs tend to share at least one terminal region across the ensemble, yielding a smoother, dense kernel.

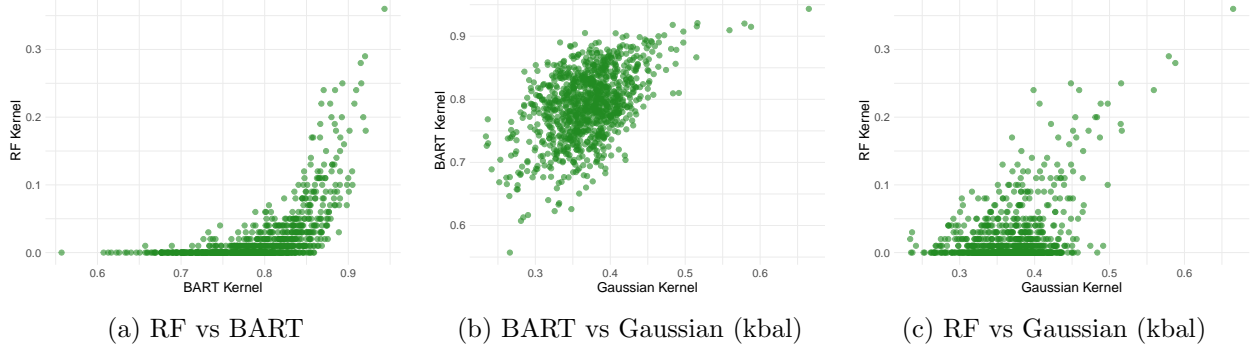


Figure 2: Comparison of RF, BART, and Gaussian kernel values. We randomly sample one unit from the observed analysis dataset and plot the corresponding kernel values on each axis.

3.2 Sample splitting and cross-fitting

While our forest kernel balancing framework uses the outcome to learn important features, this reliance alters the distinction between the design and analysis stages of causal inference: under the design principle, outcomes are not consulted during the design phase. Using the outcome for both feature construction and treatment effect estimation increases the risk of overfitting and weakens the randomized-trial analogy of observational study design ([Jin and Zubizarreta, 2025](#)). To preserve the design principle while retaining the benefits of outcome-guided kernels, we extend *sample splitting* to our forest kernel balancing approach. We require splitting the data into two samples: a *pilot sample* and an *analysis sample*.

The pilot sample is used to train the tree-ensemble model. When estimating the ATT, the pilot sample consists solely of control units so that the resulting kernel geometry targets $Y(0)$, the potential outcome we wish to learn. This model is then applied to the analysis sample, which consists of the remaining control units and the treated cohort. Specifically, we use the analysis sample to obtain the kernel matrix, solve for the weights, and estimate the treatment effect. This two-step procedure ensures the outcome is not being reused, similar to the “honest” approach of [Athey and Imbens \(2016\)](#) or the “cross-balancing” approach of [Jin and Zubizarreta \(2025\)](#). In practice, we perform this sample-splitting or cross-fitting approach multiple times to reduce the variance of the estimates, mimicking repeated cross-validation in prediction tasks. Theoretical properties of this outcome-informed approach are discussed in [Jin and Zubizarreta \(2025\)](#); we refer the reader to this manuscript for further details.

3.3 Summary: Forest Kernel Balancing

We summarize this section with a procedure for conducting forest kernel balancing. This procedure can be applied multiple times, mimicking repeated cross-fitting.

Algorithm 1 Forest Kernel Balancing

- 1: Split the data into a pilot sample (controls only for ATT) and an analysis sample.
- 2: Using the pilot sample, fit a random forest or BART model of Y^{pilot} on $\mathbf{X}^{\text{pilot}}$.
- 3: Apply the fitted model to the analysis sample to obtain the kernel matrix \mathbf{K}^{rf} or \mathbf{K}^{bart} (denote this \mathbf{K}).
- 4: Compute the spectral decomposition $\mathbf{K} = \mathbf{UDU}^{\top}$ and form the top- r eigenvectors scaled by their singular values: $\sigma_k U_k$. Any conventional selection rule can be used to select r .
- 5: If desired, augment the forest kernel with raw covariates and normalize the variance accordingly (see Section 2.3); call the resulting covariate matrix $\tilde{\Phi}$.
- 6: Estimate balancing weights using (5) with features $\tilde{\Phi}$.
- 7: Using these weights, compute the estimated ATT via (2).

Optional: repeat the procedure multiple times (cross-fitting) and aggregate the resulting estimates.

4 Simulation Studies

We conduct a simulation study, adapted from previous work on kernel balancing (Tarr and Imai, 2025), to investigate how well our forest kernel balancing methods perform relative to a design-based kernel or to balancing raw covariates alone. These simulations show that forest kernel balancing improve both bias and RMSE compared with balancing on raw covariates only or based on design-based kernel balancing.

We defer many implementation details to the appendix, which also includes results from a second simulation study based on an alternate DGP (Kim et al., 2024). All balancing weights are estimated using the `balancer` package in R, which implements the methods outlined in Ben-Michael et al. (2023) and Ben-Michael et al. (2024).

4.1 Simulation Setup

Our primary simulation DGP is from Tarr and Imai (2025), which in turn was adapted from Wong and Chan (2018); we refer to these papers for further discussion. In this simulation, both the propensity score and outcome models are nonlinear in the observed covariates and contain multiple interactions and higher order covariate transformations. Let $X = (X_1, \dots, X_{10})^{\top}$ be 10 covariates constructed to be highly nonlinear: for W_1, \dots, W_{10} iid standard Gaussians, $X_1 = \exp(W_1/2)$, $X_2 = W_2/(1+\exp(W_1))$, $X_3 = (W_1 W_3/25 + 0.6)^3$, $X_4 = (W_2 + W_4 + 20)^2$ and $X_j = W_j$ ($j = 5, \dots, 10$). The propensity score is logistic with $P(Z = 1 | W) = \text{logit}^{-1}(-W_1 - 0.1W_4)$. Finally, the outcome model is $Y(Z) = 200 + 10Z + (1.5Z - 0.5)(27.4W_1 + 13.7W_2 + 13.7W_3 + 13.7W_4) + \varepsilon$, where $\varepsilon \sim \mathcal{N}(0, 1)$. The target estimand is the ATT defined in Equation (1).

We balance on the three different feature groupings introduced in Section 3.1: raw covariates only, kernel features only, and a combination of both. For the latter two feature groupings, we balance

on a varying number of principal components to assess the sensitivity of our results to this choice. We use 1000 Monte Carlo replications and set the analysis sample size to 1000. For the pilot sample, we draw an additional sample of 1000 units and keep only the control units, resulting in roughly 500 pilot units per simulation run. We discard the treated units because our target estimand is the ATT. The random forest/BART model is trained on the pilot sample using 100 trees and the kernel is constructed by fitting this trained model to all units in the analysis sample. We measure *relative* absolute bias, defined as the absolute value of the average difference between the true treatment effect and the estimated treatment effect, divided by the true treatment effect, $|\hat{\tau} - \tau|/\tau$. We record relative absolute bias since the direction and magnitude of the bias differs for each simulation run. We also measure the *relative* root mean-squared error (RMSE), $\sqrt{(\hat{\tau} - \tau)^2/\tau}$, which we report in the main text. Results for the relative absolute bias are similar in trend and magnitude and can be found in Figure B.1 in the supplement.

4.2 Simulation Results

The relative RMSE is shown in Figure 3, plotted across a varying number of principal components (horizontal axis). An analogous plot for the relative bias can be found in Figure B.1 in the supplement. The solid lines represent different feature representations: blue represents the random forest kernel, orange represents the BART kernel, and red represents the Gaussian design-based kernel. Overall, the three kernel balancing methods exhibit similar trends in bias and RMSE across principal components. Balancing only on kernel features, however, generally performs worse than using raw covariates, especially with too few principal components. This likely reflects the fact that such a low-dimensional approximation of the kernel cannot sufficiently capture all sources of confounding. In particular, since kernel balancing emphasizes more complex interactions, this feature representation fails to account for the linear basis explained by the raw covariates.

Balancing on both the kernel features and raw covariates results in much better performance, with forest kernels outperforming the raw covariates and design-based kernel by nearly twofold for moderate numbers of included principal components. Adding more principal components continues to improve RMSE, although the gains eventually plateau for the BART and RF kernels, especially when these methods also balance the raw covariates. Across both feature groupings, the forest kernels strictly outperform the design-based kernel, demonstrating that the outcome model produces features that better capture confounding mechanisms.

In addition to evaluating estimation accuracy, we also assess the quality of the weights. In particular, we examine *the effective sample size (ESS)*:

$$\text{ESS} = \frac{(\sum_{Z_i=0} w_i)^2}{\sum_{Z_i=0} w_i^2}, \quad (7)$$

which measures loss of precision due to weight variability. In our simulation study, the ESS shows a similar pattern where the value eventually degrades when balancing on a large basis (see Figure B.2

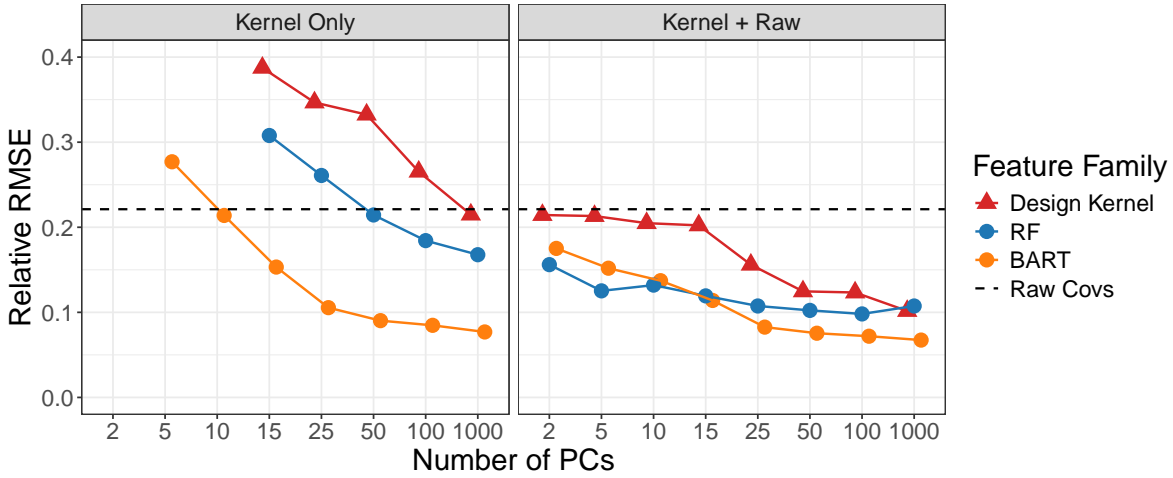


Figure 3: Absolute relative RMSE for design-based and forest kernels, varying the number of principal components to balance on. The left panel shows results using only kernel features (principal components); the right panel includes both raw features and kernel features. The black dashed line indicates performance from using raw covariates alone. Full results, including points outside the axis limits, are reported in Supplementary Table B.1.

in the supplement). These metrics suggest that our kernel balancing methods are generally robust to the number of principal components, provided the dimensionality is not pushed to extremes.

We also replicate both simulations using logistic regression to estimate the propensity score (and corresponding weights) instead of balancing weights. The results can be found in Figures B.3 and B.4 of the supplement. The substantive conclusions remain largely unchanged, indicating that our findings are not sensitive to the choice of weighting estimator.

5 Empirical Applications

We evaluate our forest kernel balancing methods using two empirical applications. The first application is a within-study comparison from [Keller et al. \(2025\)](#) that explores the relative effectiveness of a mathematics tutoring module. The second application, from [Blattman and Annan \(2010\)](#) and re-analyzed in [Wong and Chan \(2018\)](#), is an observational study of child soldiering in Uganda.

5.1 Within-Study Comparison

5.1.1 Background

We first evaluate our forest kernel balancing methods using data from [Keller et al. \(2025\)](#). This within-study comparison (WSC) design ([Wong et al., 2018](#)) allows us to directly compare estimated effects from an observational study with an experimental benchmark.

The goal of the study is to assess the impact of an instructional training module that focused on

either math or vocabulary instruction. Participants ($n = 2200$) first state a preference for math training, denoted $X_{\text{math}} = 1$, or vocabulary training, $X_{\text{math}} = 0$. Participants are then randomly assigned to math training, $Z_{\text{math}} = 1$, or vocabulary training, $Z_{\text{math}} = 0$, with randomization stratified by X_{math} . This creates four groups: $\{X_{\text{math}} = 1, Z_{\text{math}} = 1\}$ preferred math and were assigned math ($n = 288$); $\{X_{\text{math}} = 1, Z_{\text{math}} = 0\}$ preferred math and were assigned vocabulary ($n = 319$); $\{X_{\text{math}} = 0, Z_{\text{math}} = 1\}$ preferred vocabulary and were assigned math ($n = 776$); $\{X_{\text{math}} = 0, Z_{\text{math}} = 0\}$ preferred vocabulary and were assigned vocabulary ($n = 817$). While the original study included many analyses, we focus here on the impact on the math posttest, which we denote Y . We also have access to 25 baseline covariates (in addition to training preference), which we denote X .

An important feature of this within-study comparison design is that we have an experimental benchmark for the ATT of math instruction on those who would prefer math if offered the choice: $\mathbb{E}[Y(Z_{\text{math}} = 1) - Y(Z_{\text{math}} = 0) | X_{\text{math}} = 1]$. By comparing the relevant group means, [Keller et al. \(2025\)](#) found that participating in mathematics tutoring resulted in slightly higher mathematics posttest scores (0.79, SE = 0.28). The key question is whether we can replicate this experimental benchmark by instead comparing the first and fourth groups, $\{X_{\text{math}} = 1, Z_{\text{math}} = 1\}$ vs $\{X_{\text{math}} = 0, Z_{\text{math}} = 0\}$, and adjusting for the 25 baseline covariates X (excluding X_{math}).

In the supplementary materials, we present the within-study comparison for the the original covariates X , showing that all methods perform comparably to simple adjustment. In the main text, we emphasize the performance of the proposed method when covariates are highly nonlinear; following a strategy from [Hazlett \(2020\)](#), we apply an exponential transformation ($x \mapsto \log(x + 1)$) to each continuous covariate before performing the analysis. Finally, all our estimates average over ten cross-fit iterations, as in our main proposal above.

5.1.2 Results

Figure 4 shows the results from the data analysis. The experimental benchmark is indicated by the black dashed line; each estimate represents a different feature representation for balancing weights. The gray estimate shows raw covariates only, the red estimate applies the design-based Gaussian kernel ([Hazlett, 2020](#)), and blue and orange apply forest kernel balancing using random forest and BART, respectively. After inspecting a scree plot of principal components (see supplementary Figure D.3), we choose to balance on 5 principal components for illustration only (in addition to the 25 baseline covariates themselves); we find that the results are largely insensitive to the number of principal components in this example. A complete set of results across multiple principal components is reported in supplementary Figure D.1. For our analyses, we do not use cross-fitting to estimate the raw covariate and Gaussian kernel estimates, although this can be implemented if desired by the analyst.

The estimates from the transformed raw covariates and transformed Gaussian kernel deviate substantially from the experimental benchmark, with confidence intervals that nearly exclude it. In

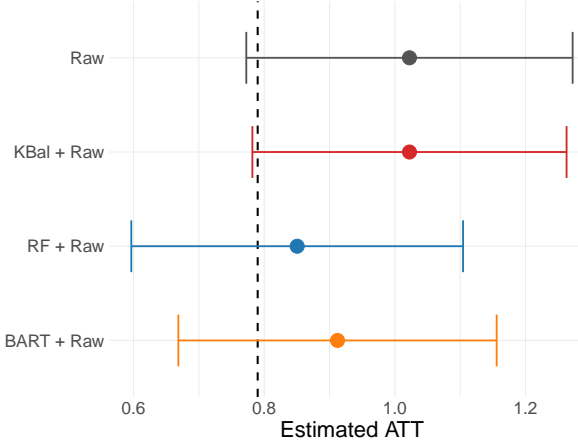


Figure 4: WSC RCT benchmarking results. The black dashed line indicates the experimental benchmark and the colored point estimates are estimated with observational data with different adjustment methods. Error bars denote 95% confidence intervals. ESS values for each feature representation are as follows: Raw: 210.9; KBal + Raw: 216; BART + Raw: 103.7; RF + Raw: 94.1 (BART and RF estimated via cross-fitting, which reduces ESS).

contrast, the forest kernel estimates are much closer to the experimental benchmark, indicating the value of using an outcome-guided approach to identify prognostic features.

5.2 Application: Forced Youth Military Service

We consider the [Blattman and Annan \(2010\)](#) study of forced youth military service in Uganda, re-analyzed by [Wong and Chan \(2018\)](#) in their seminal kernel balancing paper. In the 1980s and 1990s, there was a longstanding conflict in Northern Uganda with the Lord’s Resistance Army (LRA), a rebel group led by Joseph Kony ([Doom and Vlassenroot, 1999](#)). During this time, the LRA sustained its militia largely through indiscriminate mass abductions rather than voluntary recruitment. In a remarkable data collection effort, the 2005–2006 Survey of War Affected Youth, [Blattman and Annan \(2010\)](#) surveyed 741 males who were at risk of abduction during this conflict; of these, 462 had been previously abducted by the LRA. The authors then argue that abduction is a plausibly (conditionally) exogenous exposure: abductions occurred indiscriminately within villages and only youth within a certain age range were abducted for military service, making location and age key covariates for adjustment. Other covariates include the youth’s orphan status, household size, parental education, and amount of livestock owned.

Following [Blattman and Annan \(2010\)](#), we focus on educational attainment as the primary outcome, as measured by years of schooling. We obtain the forest kernel by averaging over ten cross-fit estimates. For each, we partition the control group ($n = 279$) into two approximately equal halves, using one half for model fitting and the other for analysis, we then swap the roles. As we discuss above, a key hyperparameter is choosing the rank of the kernel approximation to balance. Following our previous example, we examine a scree plot of principal components (see Figure C.1

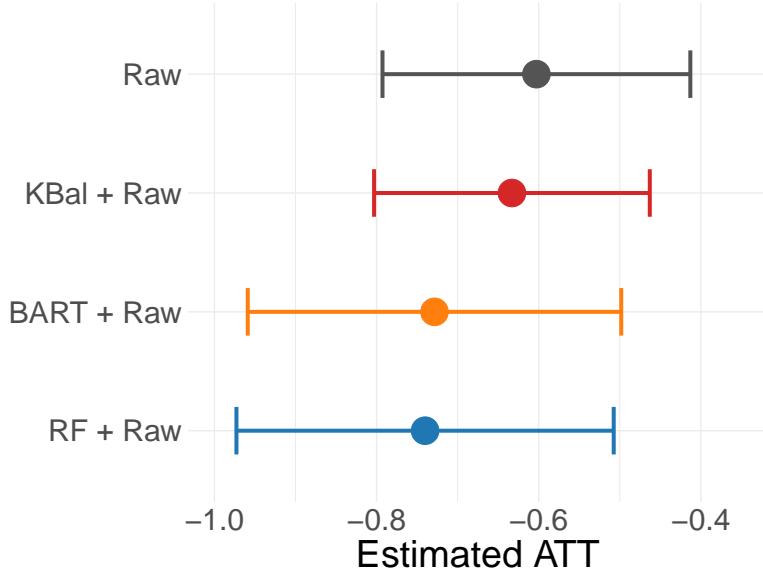


Figure 5: Child soldiering point estimates for 5 principal components. Error bars denote 95% confidence intervals. ESS values for each feature representation are as follows: Raw: 133; KBal + Raw: 171; BART + Raw: 80; RF + Raw: 78 (BART and RF estimated via cross-fitting, which reduces ESS).

in the supplement) and choose to balance on 5 principal components in addition to the 15 baseline covariates themselves.

5.2.1 Data Analysis

Figure 5 shows the results from the data analysis. Balancing the raw covariates alone and balancing both the raw covariates and the low-rank approximation to the Gaussian design-based kernel yields estimated effects of -0.6 and -0.63 years of education, respectively. By contrast, the forest kernel estimates are larger, at -0.73 and -0.74 years for BART and RF, respectively, albeit with wider confidence intervals and smaller effective sample sizes due to cross-fitting.⁴ Again, we do not use cross-fitting to estimate the raw covariate and Gaussian kernel estimates.

While there is no ground truth in this application, we can assess the stability of each method to changes in hyperparameter choice, following the “stability” principle of veridical data science (Yu, 2020; Yu and Barter, 2024; Rewolinski and Yu, 2025). Figure 6 plots the ATT estimates across a varying number of principal components, similar to the simulation study. As the number of principal components increases, the forest kernel estimates in the right-hand plot increase slightly but remain close to one another. This stability suggests that, while the RF and BART kernels have different geometries, the weights produced by each adjust for similar mechanisms of confounding. By contrast, the design-based Gaussian kernel is more sensitive to the number of principal components:

⁴The effective sample size for cross-fit Gaussian kernel balancing weights is 76, comparable to those for BART and RF.

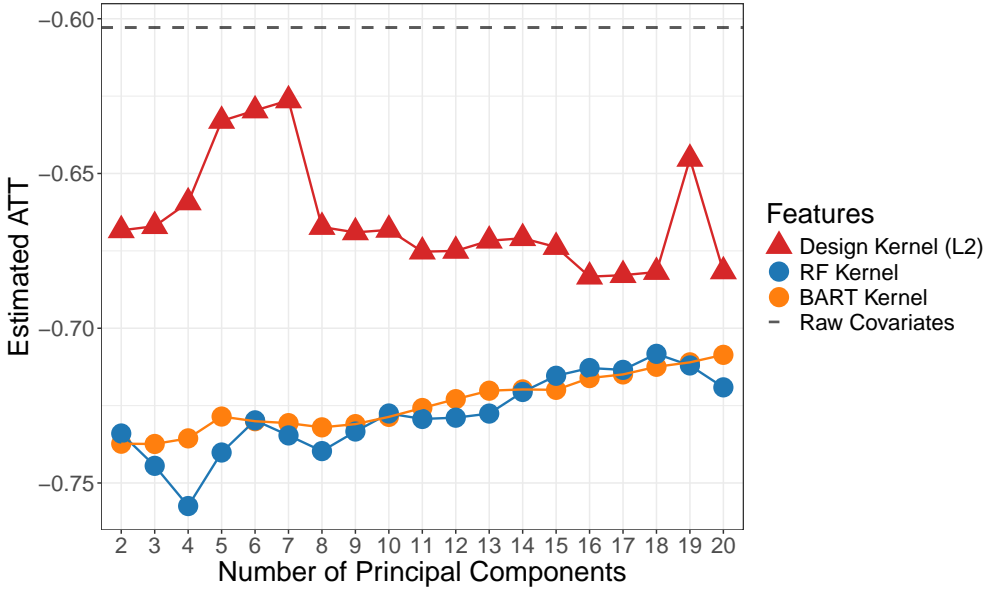


Figure 6: Estimated ATT for child soldiering across varying numbers of included principal components. These estimates balance on both raw features and kernel features. The black dashed line is the estimate from balancing using raw covariates alone.

the estimates fluctuate more noticeably as additional components are included. This behavior likely reflects the outcome-agnostic nature of design-based kernels, which encodes similarity solely on the basis of covariates rather than outcome relevance. As a result, adding more components may capture spurious variation which may or may not capture outcome-relevant confounding. The greater stability of the forest kernels suggests that incorporating outcome information helps distinguish between outcome-relevant features and those that merely reflect random covariate variation.

6 Discussion

Creating comparable groups is a key tenet of a successful observational study. Balancing weight methods seek to create such groups by producing weights that balance covariate distributions across groups. The challenge lies in correctly accounting for sources of confounding beyond raw covariates, as there exist many complex but important covariate-outcome relationships that may confound a study. In this paper, we combine principles from kernel balancing and outcome models to create an outcome-guided kernel balancing method. Specifically, we leverage the fact that random forest and BART machine learning models implicitly estimate a kernel matrix based on leaf node co-occurrences. These forest kernel matrices reflect complex relationships through the lens of the model, serving as additional features to balance on in weighting. We demonstrate how balancing on a combination of raw and kernel-based features leads to more accurate effect estimation both in simulation and in empirical studies.

There are many promising areas of future work. One is to integrate other aspects of observational

studies to the kernel balancing framework, particularly sensitivity analysis for unobserved confounding. Most sensitivity frameworks assume a linear additive basis and posit how an unobserved raw covariate may alter an observational result. Yet, as suggested by our work, the strength of unobserved confounding may also arise from covariate misspecification. Integrating feature representations with sensitivity analysis could help capture this dimension, providing a clearer view of potential threats to observational conclusions. A rich body of sensitivity analyses for weighted estimators already exists (Zhao et al., 2019; Soriano et al., 2023; Huang and Pimentel, 2025; Shen et al., 2025), so extending these frameworks to kernel balancing offers a promising line of research. Finally, our work occupies a middle ground between outcome modeling and weighting in observational studies. Another future direction is to further investigate the role of this intermediate approach as part of a broader doubly robust/augmented weighting approach (Chernozhukov et al., 2018; Bruns-Smith et al., 2025).

Acknowledgments

The authors thank Gary Chan and Raymond Wong for their assistance in obtaining the child soldiering data. A.F., L.K., and E.B-M. were supported in part by the Institute of Education Sciences (IES), U.S. Department of Education, through Grant No. R305D240036. A.S. is partially supported by the National Science Foundation (NSF) Graduate Research Fellowship under Grant No. 2146752. Any opinion, findings, and conclusions or recommendations expressed in this material are those of the authors and do not necessarily reflect the views of the IES or the NSF.

References

Agarwal, A., A. M. Kenney, Y. S. Tan, T. M. Tang, and B. Yu (2023). Mdi+: A flexible random forest-based feature importance framework. *arXiv preprint arXiv:2307.01932*.

Arbour, D., H. Parikh, B. Niknam, E. Stuart, K. Rudolph, and A. Feller (2025). Regularizing extrapolation in causal inference. *arXiv preprint arXiv:2509.17180*.

Athey, S. and G. Imbens (2016). Recursive partitioning for heterogeneous causal effects. *Proceedings of the National Academy of Sciences* 113(27), 7353–7360.

Athey, S., G. W. Imbens, and S. Wager (2018). Approximate residual balancing: debiased inference of average treatment effects in high dimensions. *Journal of the Royal Statistical Society Series B: Statistical Methodology* 80(4), 597–623.

Austin, P. C., P. Grootendorst, and G. M. Anderson (2007). A comparison of the ability of different propensity score models to balance measured variables between treated and untreated subjects: a monte carlo study. *Statistics in medicine* 26(4), 734–753.

Austin, P. C. and E. A. Stuart (2015). Moving towards best practice when using inverse probability of treatment weighting (iptw) using the propensity score to estimate causal treatment effects in observational studies. *Statistics in medicine* 34(28), 3661–3679.

Balog, M., B. Lakshminarayanan, Z. Ghahramani, D. M. Roy, and Y. W. Teh (2016). The mondrian kernel. *arXiv preprint arXiv:1606.05241*.

Ben-Michael, E., A. Feller, and E. Hartman (2024). Multilevel calibration weighting for survey data. *Political Analysis* 32(1), 65–83.

Ben-Michael, E., A. Feller, D. A. Hirshberg, and J. R. Zubizarreta (2021). The Balancing Act in Causal Inference. eprint <http://arxiv.org/abs/2110.14831>.

Ben-Michael, E., A. Feller, R. Kelz, and L. Keele (2024). Measuring racial disparities in emergency general surgery. *Journal of The Royal Statistical Society, Series A In press*.

Ben-Michael, E., A. Feller, and J. Rothstein (2023). Varying impacts of letters of recommendation on college admissions: Approximate balancing weights for subgroup effects in observational studies. *Annals of Applied Statistics* 17(4), 2843–2864.

Ben-Michael, E. and L. Keele (2023). Using balancing weights to target the treatment effect on the treated when overlap is poor. *Epidemiology* 34(5), 637–644.

Biau, G. and E. Scornet (2016). A random forest guided tour. *Test* 25(2), 197–227.

Blattman, C. and J. Annan (2010). The consequences of child soldiering. *The review of economics and statistics* 92(4), 882–898.

Breiman, L. (2000). Some infinity theory for predictor ensembles. Technical report, Technical Report 579, Statistics Dept. UCB Berkeley, CA, USA.

Breiman, L. (2001). Random forests. *Machine learning* 45, 5–32.

Bruns-Smith, D., O. Dukes, A. Feller, and E. L. Ogburn (2025). Augmented balancing weights as linear regression. *Journal of the Royal Statistical Society Series B: Statistical Methodology*, qkaf019.

Bühlmann, P. and B. Yu (2002). Analyzing bagging. *The annals of Statistics* 30(4), 927–961.

Chernozhukov, V., D. Chetverikov, M. Demirer, E. Duflo, C. Hansen, W. Newey, and J. Robins (2018, 01). Double/debiased machine learning for treatment and structural parameters. *The Econometrics Journal* 21(1), C1–C68.

Doom, R. and K. Vlassenroot (1999). Kony's message: a new koine? the lord's resistance army in northern uganda. *African affairs* 98(390), 5–36.

Gretton, A., A. Smola, J. Huang, M. Schmittfull, K. Borgwardt, B. Schölkopf, et al. (2009). Covariate shift by kernel mean matching. *Dataset shift in machine learning* 3(4), 5.

Hartman, E., C. Hazlett, and C. Sterbenz (2024). Kpop: A kernel balancing approach for reducing specification assumptions in survey weighting. *Journal of the Royal Statistical Society Series A: Statistics in Society*, qnae082.

Hazlett, C. (2020). Kernel Balancing : A flexible non-parametric weighting procedure for estimating causal effects. *Statistica Sinica* 30(3), 1155–1189.

Hill, J., A. Linero, and J. Murray (2020). Bayesian additive regression trees: A review and look forward. *Annual Review of Statistics and Its Application* 7(1), 251–278.

Hirshberg, D. and S. Wager (2021). Augmented Minimax Linear Estimation. *The Annals of Statistics* 49, 3206–3227.

Huang, M. and S. D. Pimentel (2025). Variance-based sensitivity analysis for weighting estimators results in more informative bounds. *Biometrika* 112(1), asae040.

Jin, Y. and J. Zubizarreta (2025). Cross-balancing for data-informed design and efficient analysis of observational studies. *arXiv preprint arXiv:2511.15896*.

Keele, L., E. Ben-Michael, M. Lenard, and L. Page (2025). Balancing weights for estimating treatment effects in educational studies. *Journal of Research on Educational Effectiveness*, 1–28.

Keele, L. J., E. Ben-Michael, A. Feller, R. Kelz, and L. Miratrix (2023). Hospital quality risk standardization via approximate balancing weights. *The Annals of Applied Statistics* 17(2), 901–928.

Keller, B., V. C. Wong, S. Park, J. Zhang, P. Sheehan, and P. M. Steiner (2025). A new four-arm within-study comparison: Design, implementation, and data. *Observational Studies* 11(2), 153–188.

Kim, K., B. A. Niknam, and J. R. Zubizarreta (2024). Scalable kernel balancing weights in a nationwide observational study of hospital profit status and heart attack outcomes. *Biostatistics* 25(3), 736–753.

Lin, Y. and Y. Jeon (2006). Random forests and adaptive nearest neighbors. *Journal of the American Statistical Association* 101(474), 578–590.

Rewolinski, Z. T. and B. Yu (2025). Pcs workflow for veridical data science in the age of ai. *arXiv preprint arXiv:2508.00835*.

Rubin, D. B. (1986, December). Which ifs have causal answers. *Journal of the American Statistical Association* 81(396), 961–962.

Scornet, E. (2016). Random forests and kernel methods. *IEEE Transactions on Information Theory* 62(3), 1485–1500.

Shen, A. A., E. Visoki, R. Barzilay, and S. D. Pimentel (2025). A calibrated sensitivity analysis for weighted causal decompositions. *Statistics in medicine* 44(5), e70010.

Soriano, D., E. Ben-Michael, P. J. Bickel, A. Feller, and S. D. Pimentel (2023). Interpretable sensitivity analysis for balancing weights. *Journal of the Royal Statistical Society Series A: Statistics in Society* 186(4), 707–721.

Tan, Z. (2020). Regularized calibrated estimation of propensity scores with model misspecification and high-dimensional data. *Biometrika* 107(1), 137–158.

Tarr, A. and K. Imai (2025). Estimating average treatment effects with support vector machines. *Statistics in Medicine* 44(5), e70006.

Wager, S. and S. Athey (2018). Estimation and inference of heterogeneous treatment effects using random forests. *Journal of the American Statistical Association* 113(523), 1228–1242.

Wang, Y. and J. R. Zubizarreta (2020). Minimal dispersion approximately balancing weights: asymptotic properties and practical considerations. *Biometrika* 107(1), 93–105.

Welz, M., A. Alfons, M. Demirer, and V. Chernozhukov (2024). *GenericML: Generic Machine Learning Inference*. R package version 0.2.2.

Wong, R. K. and K. C. G. Chan (2018). Kernel-based covariate functional balancing for observational studies. *Biometrika* 105(1), 199–213.

Wong, V. C., P. M. Steiner, and K. L. Anglin (2018). What can be learned from empirical evaluations of nonexperimental methods? *Evaluation review* 42(2), 147–175.

Yu, B. (2020). Veridical data science. In *Proceedings of the 13th international conference on web search and data mining*, pp. 4–5.

Yu, B. and R. L. Barter (2024). *Veridical data science: The practice of responsible data analysis and decision making*. MIT Press.

Zhao, Q., D. S. Small, and B. B. Bhattacharya (2019). Sensitivity analysis for inverse probability weighting estimators via the percentile bootstrap. *Journal of the Royal Statistical Society Series B: Statistical Methodology* 81(4), 735–761.

Zubizarreta, J. R. (2015). Stable weights that balance covariates for estimation with incomplete outcome data. *Journal of the American Statistical Association* 110(511), 910–922.

Supplementary Materials:

Forest Kernel Balancing Weights: Outcome-Guided Features for Causal Inference

A Additional figures

Figure A.1 provides a simple illustration of the first two principal components (PCs) of the RF (A.1a) and BART (A.1b) kernels. The plots come from the same realization of the DGP used to present Figure 2 in the main text. We note that different DGPs (and even different draws of the same DGP) can produce qualitatively different PC configurations.

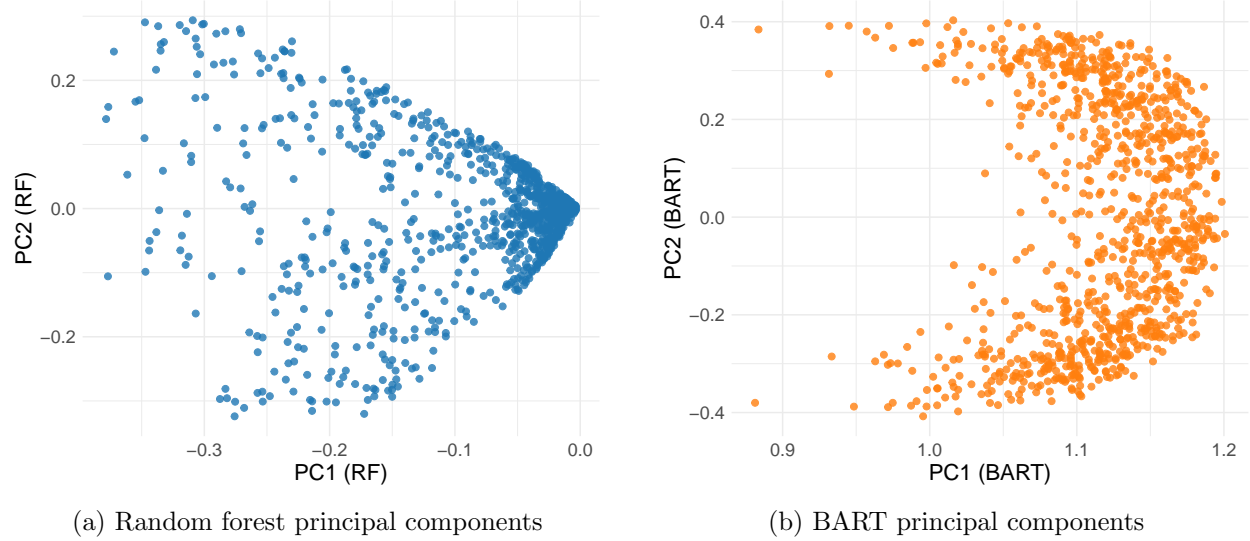


Figure A.1: Side-by-side comparison of random forest (left) and BART (right) principal-component scatterplots.

B Additional results from Simulation 1

In this section, we present additional results from Simulation 1 (in the main text) that were omitted for clarity.

B.1 Full bias and RMSE results

Figure B.1 shows the relative bias from this simulation, analogous to Figure 3 in the main text.

Table B.1 shows the results from the figure in Section 4 the main text. As certain points were

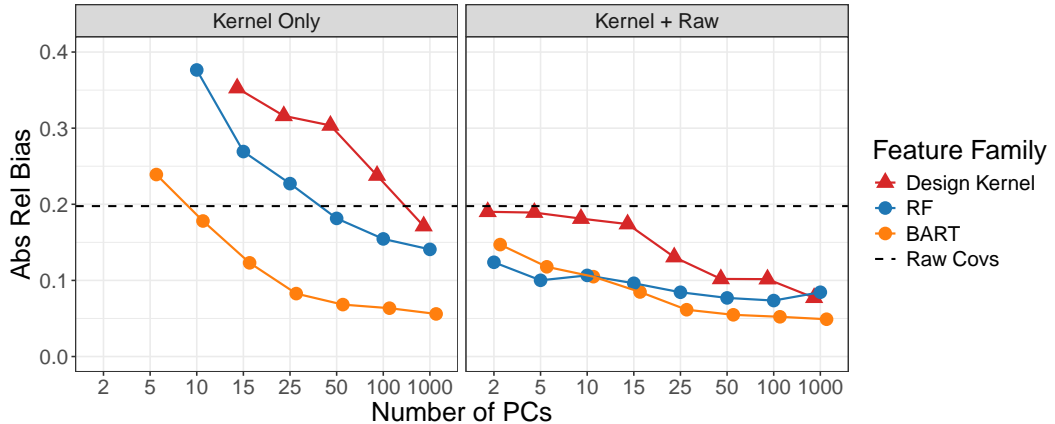


Figure B.1: Absolute relative bias for design-based and forest kernels, varying the number of principal components to balance on. The left panel shows results using only kernel features (principal components); the right panel includes both raw features and kernel features. The black dashed line indicates performance from using raw covariates alone. Full results, including points outside the axis limits, are reported in Supplementary Table B.1.

omitted from the plot due to large bias/RMSE magnitudes, this table is presented for completeness.

B.2 Balance metrics

Figure B.2 displays the effective sample sizes (ESS) for the first simulation study. Discussion of this metric can be found in Section 4 of the main manuscript.

B.3 Weight estimation with logistic regression

In Figures B.3 and B.4, we present results from the first simulation using logistic regression to estimate the propensity score instead of direct estimation with balancing weights. The substantive conclusions remain the same as those in the main manuscript, indicating that the method for weight estimation is not critical in the forest kernel balancing framework.

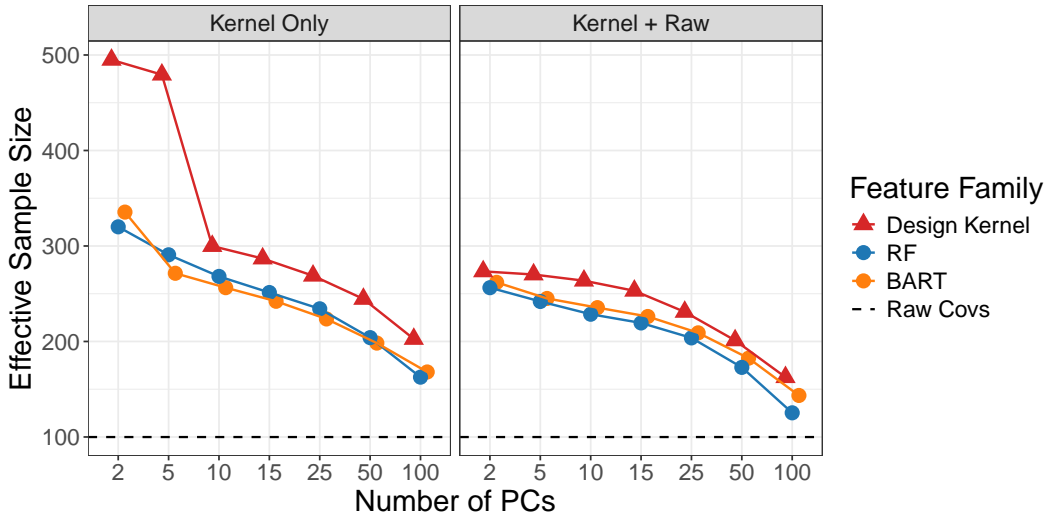


Figure B.2: Effective sample size for design-based and forest kernels, varying the number of principal components to balance on. The left panel shows results using only kernel features (principal components); the right panel includes both raw features and kernel features. The black dashed line indicates ESS from using raw covariates alone.

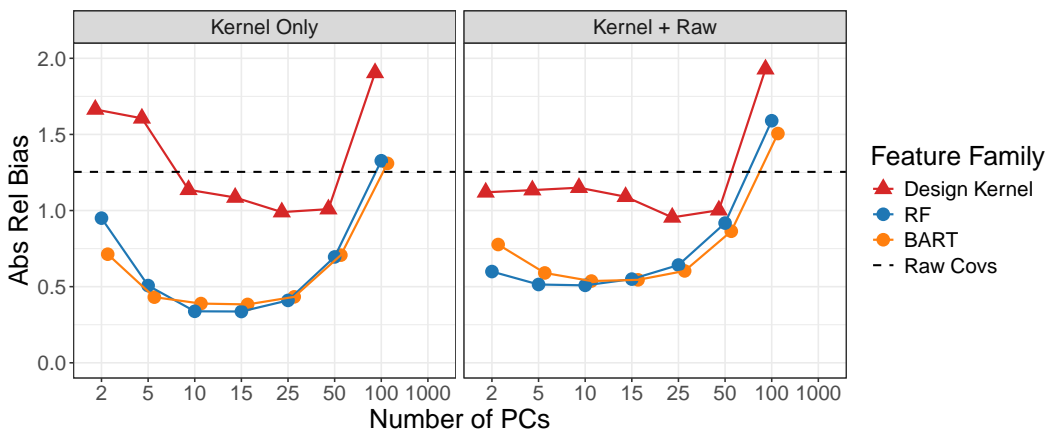


Figure B.3: Results when logistic regression is used for weight estimation instead of balancing weights. We plot absolute relative bias for design-based and forest kernels, varying the number of principal components to balance on. The left panel shows results using only kernel features (principal components); the right panel includes both raw features and kernel features. The black dashed line indicates performance from using raw covariates alone.

| Feature Grouping | Number of PCs | Absolute Bias | Relative RMSE |
|------------------|---------------|---------------|---------------|
| bart_only | 2.00 | 0.61 | 0.99 |
| bart_only | 5.00 | 0.23 | 0.27 |
| bart_only | 10.00 | 0.17 | 0.22 |
| bart_only | 15.00 | 0.12 | 0.15 |
| bart_only | 25.00 | 0.08 | 0.10 |
| bart_only | 50.00 | 0.07 | 0.09 |
| bart_only | 100.00 | 0.06 | 0.08 |
| bart_plus | 2.00 | 0.14 | 0.17 |
| bart_plus | 5.00 | 0.11 | 0.15 |
| bart_plus | 10.00 | 0.10 | 0.13 |
| bart_plus | 15.00 | 0.08 | 0.10 |
| bart_plus | 25.00 | 0.06 | 0.08 |
| bart_plus | 50.00 | 0.05 | 0.07 |
| bart_plus | 100.00 | 0.05 | 0.07 |
| kbal_only | 2.00 | 1.63 | 1.79 |
| kbal_only | 5.00 | 1.59 | 1.74 |
| kbal_only | 10.00 | 0.40 | 0.46 |
| kbal_only | 15.00 | 0.35 | 0.40 |
| kbal_only | 25.00 | 0.31 | 0.36 |
| kbal_only | 50.00 | 0.30 | 0.35 |
| kbal_only | 100.00 | 0.23 | 0.27 |
| kbal_plus | 2.00 | 0.19 | 0.22 |
| kbal_plus | 5.00 | 0.19 | 0.22 |
| kbal_plus | 10.00 | 0.18 | 0.21 |
| kbal_plus | 15.00 | 0.17 | 0.21 |
| kbal_plus | 25.00 | 0.13 | 0.16 |
| kbal_plus | 50.00 | 0.10 | 0.13 |
| kbal_plus | 100.00 | 0.10 | 0.13 |
| raw | 0.00 | 0.20 | 0.23 |
| rf_only | 2.00 | 0.52 | 0.57 |
| rf_only | 5.00 | 0.48 | 0.53 |
| rf_only | 10.00 | 0.37 | 0.42 |
| rf_only | 15.00 | 0.25 | 0.29 |
| rf_only | 25.00 | 0.22 | 0.25 |
| rf_only | 50.00 | 0.17 | 0.20 |
| rf_only | 100.00 | 0.15 | 0.18 |
| rf_plus | 2.00 | 0.12 | 0.15 |
| rf_plus | 5.00 | 0.10 | 0.12 |
| rf_plus | 10.00 | 0.10 | 0.13 |
| rf_plus | 15.00 | 0.09 | 0.12 |
| rf_plus | 25.00 | 0.08 | 0.10 |
| rf_plus | 50.00 | 0.07 | 0.09 |
| rf_plus | 100.00 | 0.07 | 0.09 |

Table B.1: Complete balancing weight results from simulation 1. Feature representations with `_only` are kernel only features, `_plus` are kernel + raw covariates.

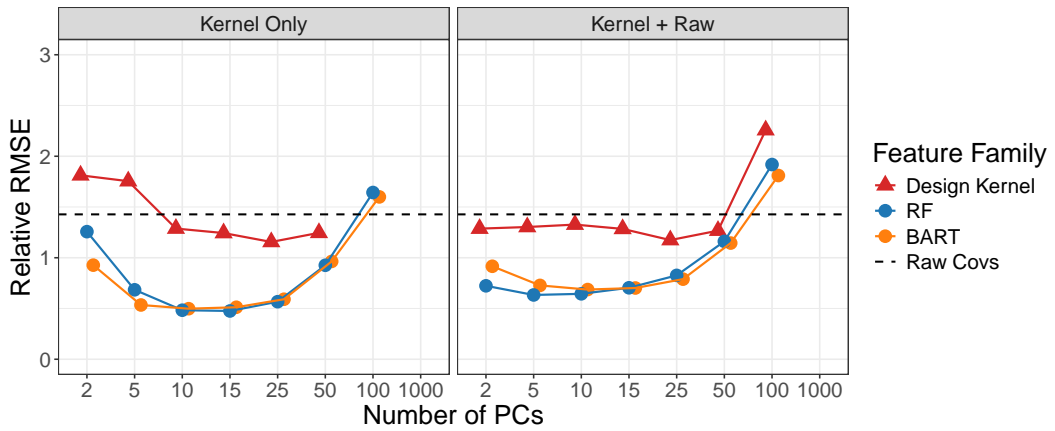


Figure B.4: Results when logistic regression is used for weight estimation instead of balancing weights. We plot absolute relative RMSE for design-based and forest kernels, varying the number of principal components to balance on. The left panel shows results using only kernel features (principal components); the right panel includes both raw features and kernel features. The black dashed line indicates performance from using raw covariates alone.

C Additional results from child soldiering study

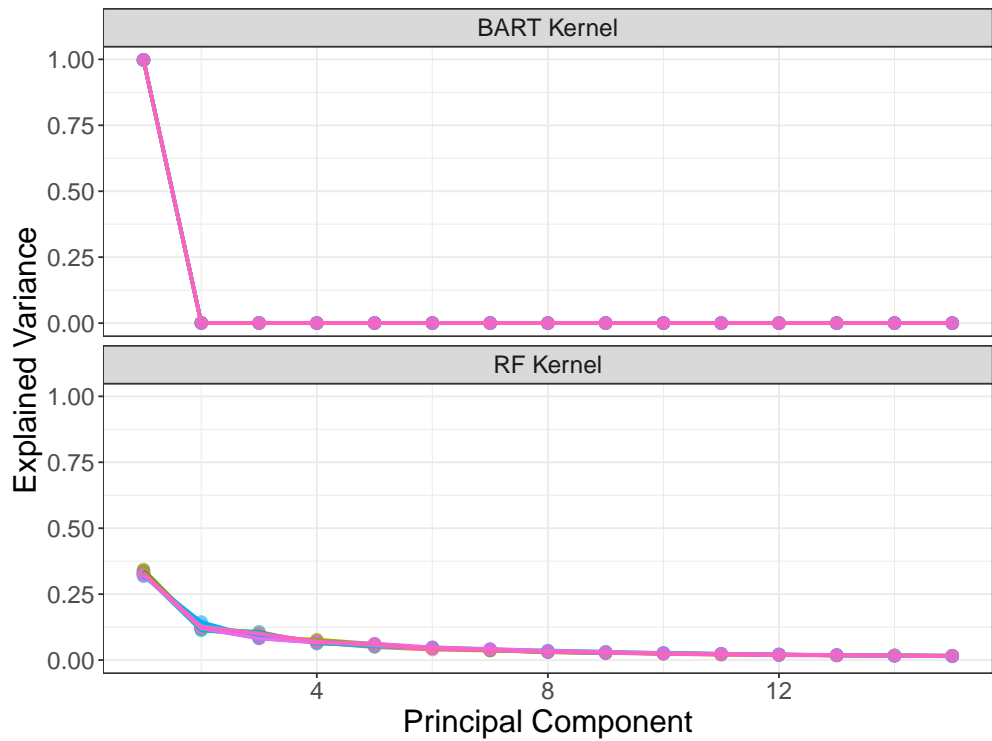


Figure C.1: Scree plot of principal components for BART and RF kernels for child soldiering study for all ten cross-fit folds. We plot the principal component on the horizontal and the corresponding explained variance on the vertical axis.

D Additional results from within-study comparison

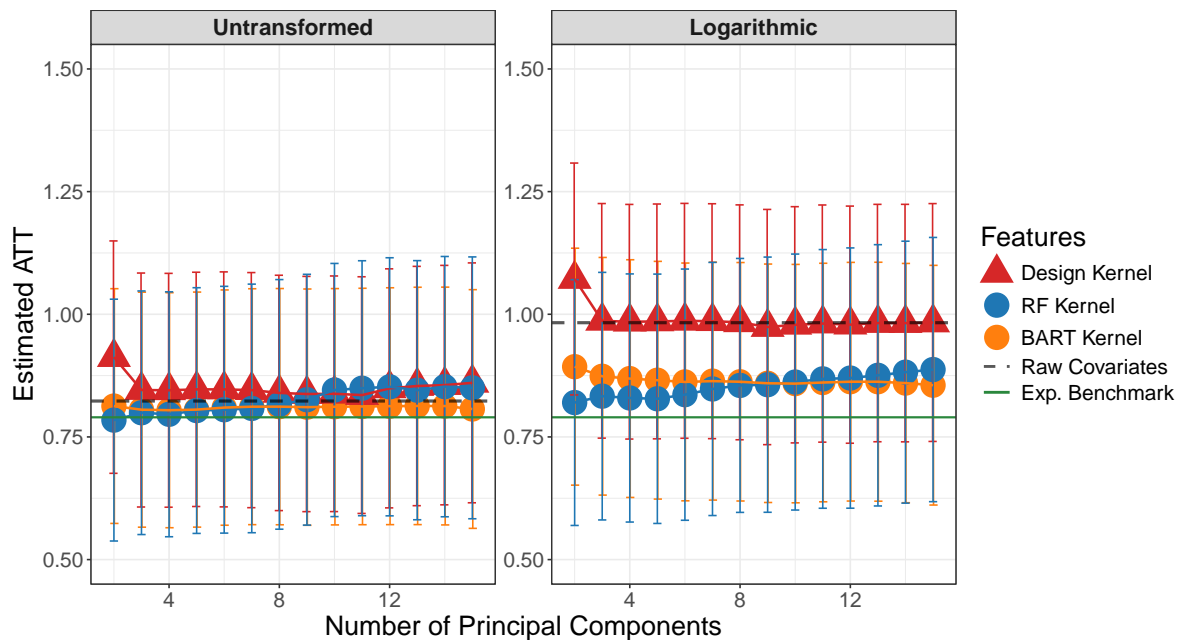


Figure D.1: Full results for WSC empirical study with exponential ($\log(x + 1)$) covariate transformation. We plot the estimated ATT over a range of principal components (PCs) for kernel balancing methods. All points adjust for raw covariates and the specified number of PCs. The black dashed line is the estimate from using raw covariates only. The green solid line is the experimental benchmark.

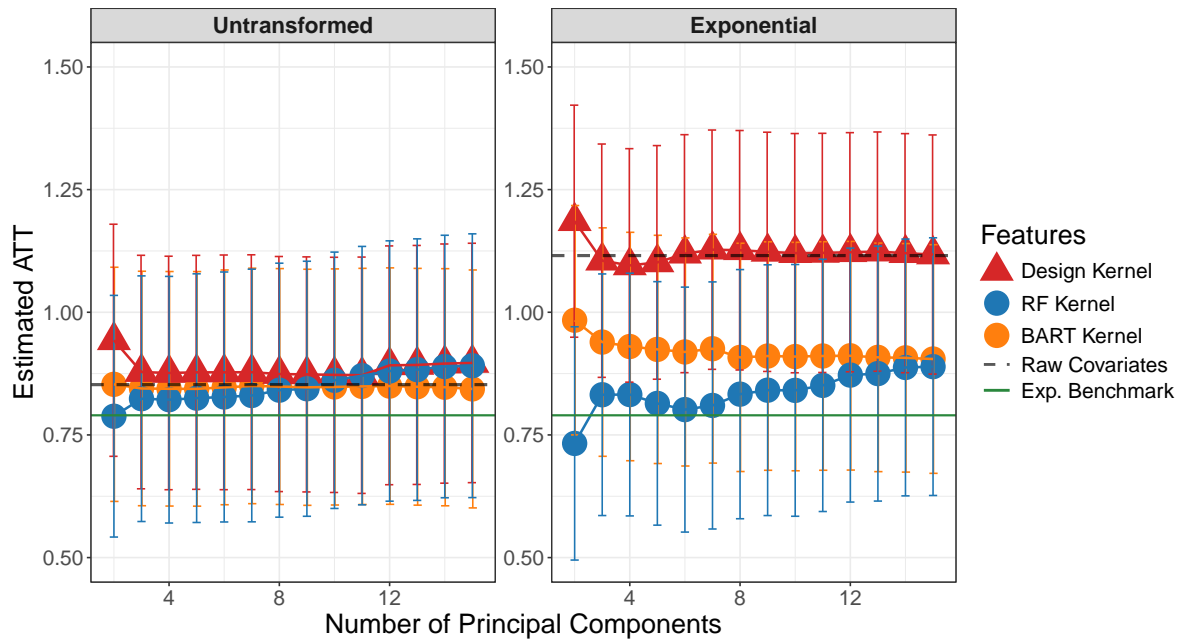


Figure D.2: Full results for WSC empirical study with exponential ($\exp(x)$) covariate transformation. We plot the estimated ATT over a range of principal components (PCs) for kernel balancing methods. All points adjust for raw covariates and the specified number of PCs. The black dashed line is the estimate from using raw covariates only. The green solid line is the experimental benchmark.

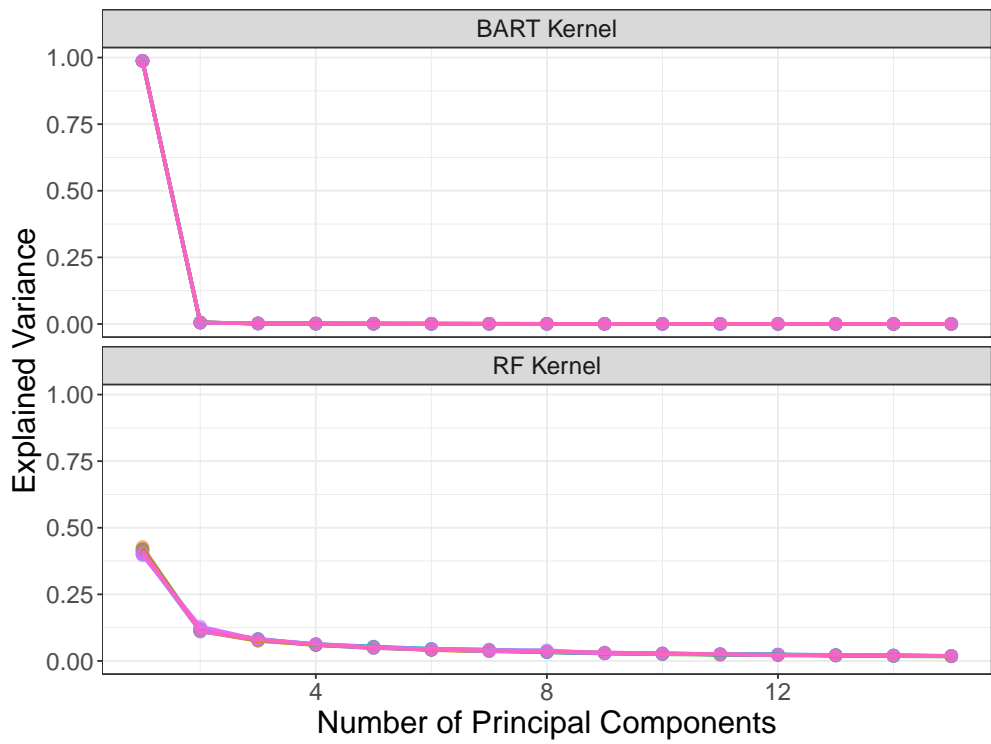


Figure D.3: Scree plot of principal components for BART and RF kernels for within-study comparison for all ten cross-fit folds. We plot the principal component on the horizontal and the corresponding explained variance on the vertical axis.

E Additional simulation study

E.1 Simulation setup

The second simulation is adapted from [Kim et al. \(2024\)](#). This DGP also represents a highly nonlinear scenario in both the propensity score and the outcome model. In addition, we also control the overlap between treated and control groups (defined below).

In this simulation, we construct the following observed covariates:

$$\begin{bmatrix} X_1 \\ X_2 \\ X_3 \end{bmatrix} \sim N \left(\begin{bmatrix} 0 \\ 0 \\ 0 \end{bmatrix}, \begin{bmatrix} 2 & 1 & -1 \\ 1 & 1 & -0.5 \\ -1 & -0.5 & 1 \end{bmatrix} \right), \quad X_4 \sim \text{Unif}[-3, 3], \quad X_5 \sim \chi_1^2, \quad X_6 \sim \text{Bern}[0.5].$$

The treatment Z and outcome Y are generated as

$$Z_i = \mathbb{1} \left\{ X_{i1}^2 + 2X_{i2}^2 - 2X_{i3}^2 - (X_{i4} + 1)^3 - 0.5 \log(X_{i5} + 10) + X_{i6} - 1.5 + \varepsilon_i > 0 \right\}, \quad \varepsilon_i \sim \mathcal{N}(0, \sigma_\varepsilon^2),$$

$$Y_i = (X_{i1} + X_{i2} + X_{i5})^2 + \eta_i, \quad \eta_i \sim \mathcal{N}(0, 1).$$

Following [Kim et al. \(2024\)](#), we consider $\sigma_\varepsilon^2 = 30$ and $\sigma_\varepsilon^2 = 100$, corresponding to the *low* and *high overlap* settings, respectively. Observe that the ATT is equal to 0 by construction.

Following the setup in the main manuscript, we compare the performance of forest kernel balancing weights against a design-based Gaussian kernel and balancing on raw covariates only. The results are included in Figures E.1 (bias) and E.2 (RMSE).

Figures E.3 and E.4 below display results for this simulation study when logistic regression is used for weight estimation instead of balancing weights.

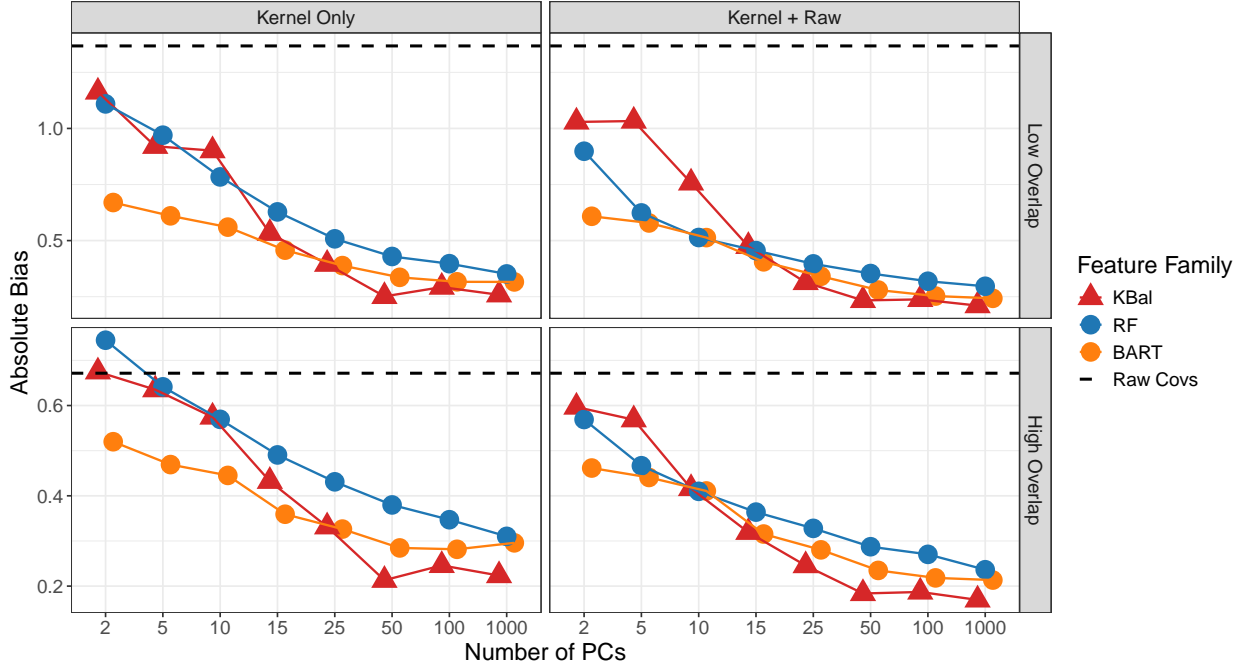


Figure E.1: Bias plot for design-based and forest kernels, varying the number of principal components to balance on. The left panel shows results using only kernel features (principal components); the right panel includes both raw features and kernel features. The black dashed line indicates performance from using raw covariates alone.

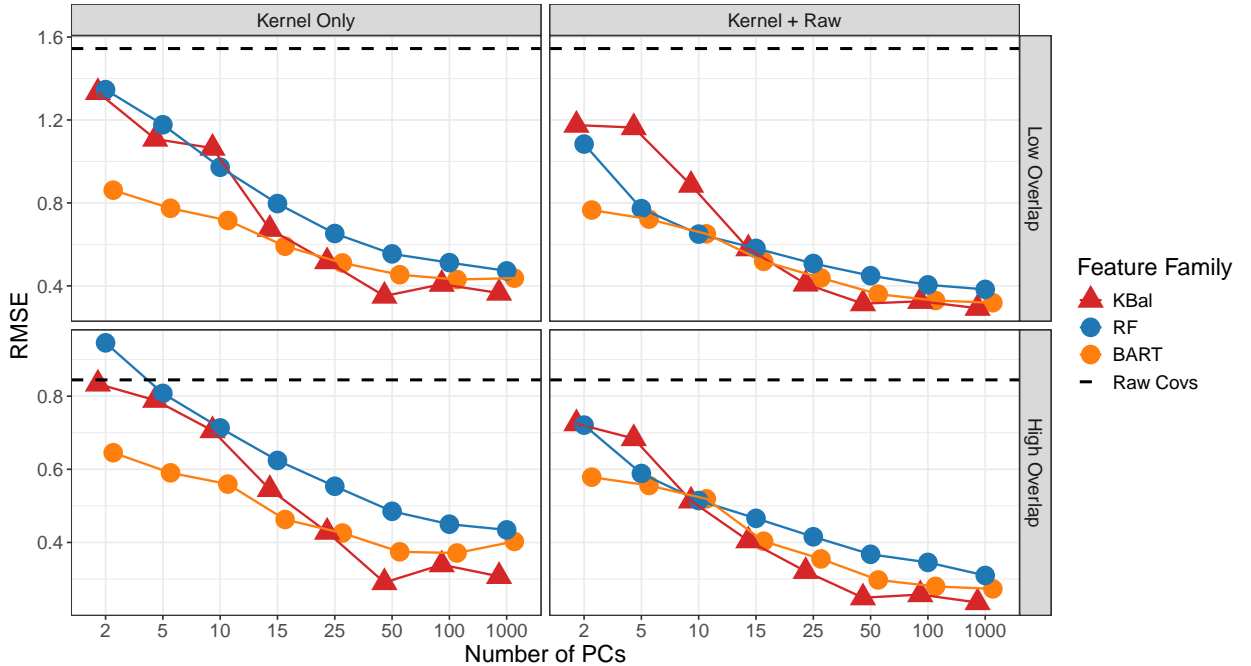


Figure E.2: RMSE plot for design-based and forest kernels, varying the number of principal components to balance on. The left panel shows results using only kernel features (principal components); the right panel includes both raw features and kernel features. The black dashed line indicates performance from using raw covariates alone.

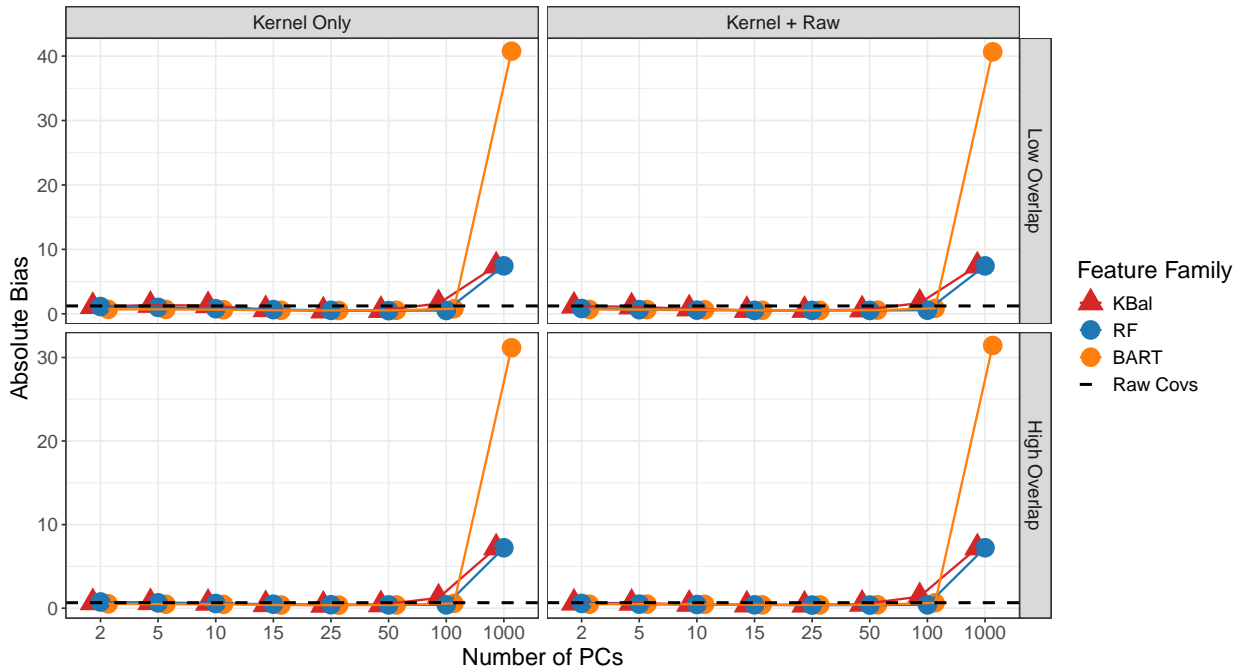


Figure E.3: Results when logistic regression is used for weight estimation instead of balancing weights. We plot absolute bias for design-based and forest kernels, varying the number of principal components to balance on. The left panel shows results using only kernel features (principal components); the right panel includes both raw features and kernel features. The black dashed line indicates performance from using raw covariates alone.

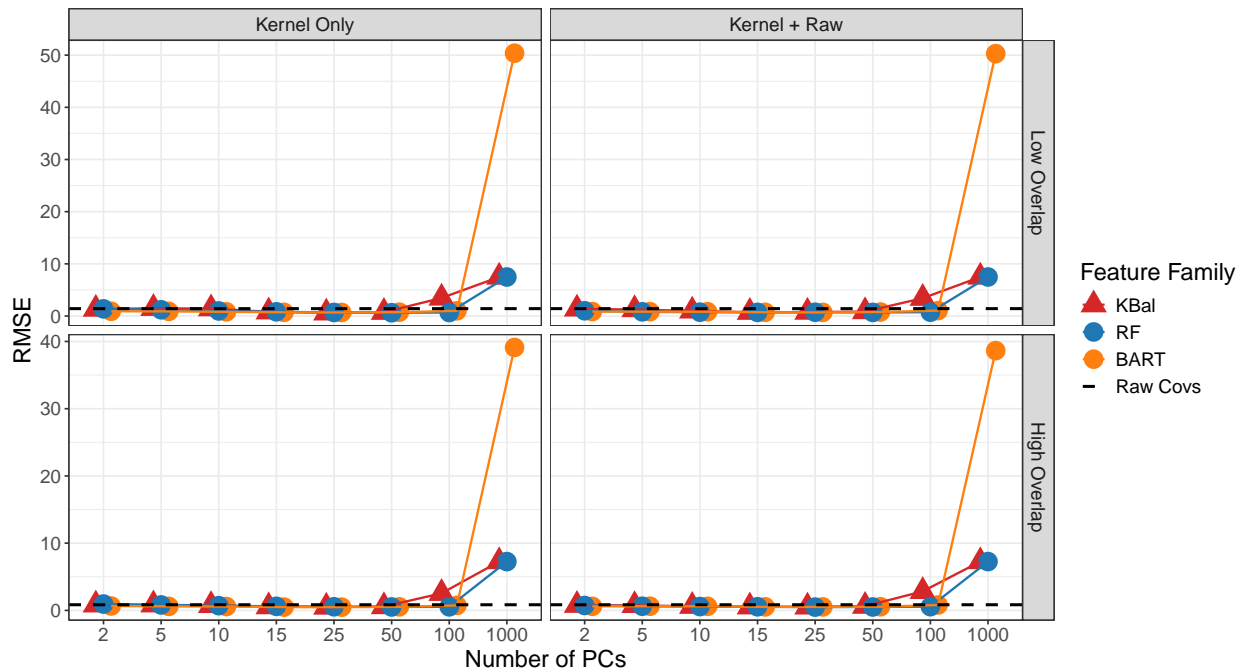


Figure E.4: Results when logistic regression is used for weight estimation instead of balancing weights. We plot RMSE for design-based and forest kernels, varying the number of principal components to balance on. The left panel shows results using only kernel features (principal components); the right panel includes both raw features and kernel features. The black dashed line indicates performance from using raw covariates alone.